

MR Imaging of Pancreatic Islets: Tracking Isolation, Transplantation and Function

L. Leoni¹ and B.B. Roman^{1,2,3*}

¹Department of Radiology, ²Committee on Medical Physics, ³Committee on Metabolism and Nutrition, University of Chicago, Chicago, IL, USA

Abstract: The increasing global incidence of diabetes and advancements in clinical pancreatic islet transplantation for the treatment of Type I diabetes have renewed the interest in understanding the variations of β -cell mass and function relative not only to transplant outcome but also to the onset and progression of diabetes. A deeper comprehension of the molecular and cellular processes involved in pancreatic islet inflammation and cytotoxicity is necessary to further improve efficacy of islet transplantation and to develop new therapies aimed at preserving beta cell function in pathological conditions. Available diagnostic methods based on metabolic response are unsuitable as they lack correlation to islet mass, viability and function. Great emphasis has been placed on developing noninvasive imaging technologies which enable the tracking of both endogenous and transplanted islet mass and potentially function overtime, the characterization of changes in islet vasculature and the degree of T-cell infiltration during insulinitis.

Among the more relevant modalities are magnetic resonance, positron emitted tomography, single photon emission computed tomography, bioluminescence and fluorescence optical imaging. This review focuses on the most recent advancements in magnetic resonance imaging (MRI) of pancreatic islets. *In-vitro* approaches aimed at characterizing the potency of isolated islets as well as *in-vivo* advancements in the assessment of transplanted beta cell mass are presented together with the significant progress made in the *in-vivo* imaging of the endocrine pancreas and islet vasculature and inflammation. Different experimental approaches are compared via their advantages and limitations with respect to their clinical implementation.

Keywords: Beta cell function, contrast agents, *in vivo* imaging, magnetic resonance imaging, pancreatic islets.

INTRODUCTION

Regulation of blood glucose concentrations requires an adequate number of functional pancreatic β -cells able to respond to fluctuating glucose levels. Type I diabetes is a chronic autoimmune disease characterized by a targeted inflammatory reaction against insulin secreting β -cells. This process results in a gradual loss of β -cells and eventually in overt diabetes requiring insulin replacement therapy in order to maintain physiological levels of blood glucose. Pancreatic islet transplantation has shown promise in restoring near normal glucose control in selected Type I diabetes patients although a 5 years follow-up showed only 10-15% rate of insulin independency [1]. Therefore a better understanding of the factors involved in islet graft survival is necessary to establish islet transplantation as a reliable therapy.

Although more manageable in the initial phase, Type II diabetes, which is due to both insulin deficiency and insulin resistance, also requires pharmacological treatment in the long term. Interventional therapies aimed at preserving and expanding the remaining β -cell mass are complicated by the fact that most of the knowledge of the total pancreatic β -cell mass in humans comes from autopsy studies [2-5] and therefore represents endpoint assessments and provide no functional information. Similarly, serological assays of insulin secretory response have shown no correlation with morphometric β -cell mass nor quantitatively reflect β -cell function [6].

Relevant information on β -cell mass and function that will help understanding diabetes, improve current therapies and develop new approach are most likely to come from a multidisciplinary comprehensive approaches. Noninvasive imaging technologies have been playing a major role in this effort and are considered a high priority as shown by the increasing number of review papers published in the last few years [7-13]. Magnetic resonance imaging (MRI) of pancreatic islets has seen very encouraging developments some of which are currently being translated into clinical trials.

These and other more experimental MRI techniques will be described in this review.

GENERAL MRI CONSIDERATIONS

MRI is a desirable modality as it involves the use on non-ionizing radiation and has virtually no side effects. It has excellent soft tissue contrast resolution and can image multiple planes and is therefore able to render tomographic reconstructions. MRI is also capable of targeting a number of useful pathophysiological variables at the microscopic, cellular and potentially molecular level. However, it suffers inherently from a lack of sensitivity and specificity to pancreatic islet mass and function compared to other imaging modalities. A healthy pancreas is estimated to contain about one million pancreatic islets accounting for approximately 1-2% of the organ volume of which insulin secreting β -cells make up only about 60-80% [14]. Furthermore islets are scattered throughout the whole pancreas and although their size distribution varies between 50 and 500 μm , they average 100-150 μm in diameter [15-17]. Pancreatic tissue density decreases even further during the onset and progression of diabetes. Detecting the actual functional mass is even more challenging, as not all pancreatic islets are believed to be simultaneously activated and they could have different degree of response when stimulated.

Although MR images display excellent inherent contrast, exogenous agents are often infused to enhance specific anatomical and functional tissue characteristics. Contrast agents play an essential role in sensitizing MRI to β -cell mass and function. They induce contrast changes by shortening T1 or T2 and T2* relaxation times of nearby water protons which translates into hyperintense regions in T1-weighted images or hypointense regions in T2 weighted images. T2* agents, namely iron-oxide nanoparticles, have shown the most utility and have rapidly moved from animal models to clinical applications ([11, 18, 19]). They consist of a water insoluble crystalline magnetic core ranging from 4 to about 50 nm in diameter and encased into a layer of dextran or other biocompatible polymers that can be chemically modified to increase cellular specificity and uptake efficiency. These particles are used to label isolated pancreatic islets *ex-vivo* and to follow them *in-vivo* after transplantation. The evidence indicates that iron uptake by islets is an endocytic process based on low affinity

*Address correspondence to this author at the Department of Radiology, MC2026, University of Chicago, 5841 S. Maryland Ave., Chicago, IL, 60637, USA; Tel: 773-702-6906; Fax: 773-702-1161; E-mail: broman@uchicago.edu

processes with varying labeling efficiencies which are dependent on, among other factors, the amount of iron per IEQ and on the type of supermagnetic iron oxide (SPIO) considered [20-26]. Once taken up, particles are stored in endosomes for several days allowing for long-term monitoring. Although *in-vitro* studies have shown good correlation between MR signal and islet mass [19, 27, 28], *in-vivo* studies still lack such correspondence. This is due to several factors. It is estimated that about 10% of the SPIO in an islet are not intracellular but rather residing in the islet stroma. Also, dead islets seem to retain SPIOs for some time and therefore in both cases the hypointense iron signal would not be linked to the actual presence of viable islets [25, 26, 29]. More importantly, the fate of iron particles released into the liver by dying islets poses some issues. According to data presented by Evgenov *et al.* [27], immune cells infiltrating into transplanted islets in a NOD mouse model did not internalize SPIOs. Rather, iron particles were released into the liver parenchyma, internalized by Kupffer cells and rapidly cleared from the organ. Therefore no false positive due to free iron particles would be present in MR images. However several studies involving *in-vivo* monitoring of transplanted mesenchymal stem cells (MSC) in different organs have reported iron particles being engulfed by macrophages and consequently a pronounced mismatch between the hypointense MR signal and the labeled cells [25, 26, 30]. This has been recently confirmed in a rat model where most of the hypointense regions observed in the liver 42 days after islet transplantation were correlated with iron aggregates accumulated mainly in macrophages [29]. The first reported clinical study also emphasized issues related to endogenous iron levels in the liver. Two out of the four patients in the study had high iron concentrations and consequently their MR images had such a high background signal rendering MR image analysis impossible [18]. Nonetheless, at the moment MR imaging of SPIO labeled islets remains one of the most promising technologies for MR imaging of islet grafts.

To avoid the limitations associated with iron, some groups are turning to alternative compounds such as fluorine-19 (^{19}F) and more common T_1 contrast agents which give an increase on signal intensity in the islet instead of the decrease caused by T_2 agents. ^{19}F has been used recently in the form of perfluoropolyether (PFPE) nanoparticles for MR imaging of *ex-vivo* labeled cell migration [31, 32]. Advantages of using ^{19}F include high signal specificity and lack of background signal due to below detection levels of fluorine in the body thus making absolute cell quantitation possible. Moreover, PFPE has no known intracellular biological reactivity and is not degraded *in vivo* allowing for longitudinal studies [31, 32].

Gadolinium-diethylenetriaminepentaacetic acid (GdDTPA) is an FDA approved T_1 agent commonly used in clinical MRI. Different Gd complexes have been synthesized and have shown some potential as labeling agents, similarly to iron particles [33], and as a vascular tracer in models of islet inflammation as well as in islet kidney transplants [34, 35]. Because of its inherent lack of sensitivity, different approaches have been undertaken to increase its relaxivity, that is its ability to enhance MR signal in T_1 -weighted images. Multiple Gd chelates have been attached to a modified benzene template resulting in a contrast agent with a five fold increase in relaxivity than clinical Gd based compounds [36]. Moreover this agent has sites available to attach specific cell targeting or labeling groups to increase efficiency of islet labeling and longevity *in vivo*. Preliminary *in-vitro* tests have yielded positive results however *in-vivo* data is not yet available.

Manganese (Mn) is another T_1 contrast agent that has been attracting more interest. Mn is an excellent MR contrast agent due to its T_1 relaxation properties [37-41] and was used as the first MRI contrast agent by Lauterbur and coworkers [42] and it has the intrinsic ability of visualizing beta cell activation by sensitizing MRI to calcium influx and as such it is so far the only contrast agent directly linked to beta cell functionality. Mn has an ionic

radius similar to that of calcium, and is handled similarly in many biological systems [43]. Divalent manganese ions (Mn^{2+}) enter beta cells through voltage-gated calcium channels [44] which open in response to a rise in extracellular glucose and the subsequent closure of ATP-sensitive K^+ channels. Therefore, Mn can be used not only *in-vitro* to characterize isolated islet potency but more importantly *in vivo* to assess the functionality of both grafted and endogenous pancreatic islets [45-47]. As with other contrast agents, Mn has some limitations mainly linked to its lack of specificity towards beta cells and its potential cytotoxicity.

Non-invasive pancreatic imaging is still in its infancy and as new biomarkers specific to beta cells are discovered, new more specific contrast agents able to sensitize MRI to β -cell function will become available. In addition to specificity, pancreatic MRI has to deal with the anatomic location of the pancreas. Close proximity of the pancreas to the stomach and intestines, complicates detection due to similar tissue characteristics/density and benefits from tissue suppression pulse sequences to decrease contributions from non-pancreatic tissues. Artifacts arising from respiratory motion are also problematic which further lower MRI sensitivity and therefore require longer acquisition times. Continuous hardware and software improvements have contributed to minimizing these artifacts by shortening experimental times. Some of these advances however cannot yet be translated to the clinical setting where lower magnetic fields are used.

MRI OF ISOLATED AND TRANSPLANTED PANCREATIC ISLETS

The two major challenges raised by clinical islet transplantation are the assessment of the mass and functionality of isolated islets both prior to and post transplantation. Optical imaging methods as well as biochemical and metabolic assays are currently used to evaluate islet viability and potency. We have recently showed that MRI can be used to evaluate isolated human islets *in-vitro*. As shown in Fig. 1, using Mn as a reporter we were able to link its intracellular uptake and image contrast enhancement in T_1 -weighted images to pancreatic beta cell activation [48, 49]. Isolated islets were loaded in a perfusion system designed to fit inside the magnet and were continuously perfused with $50\mu\text{M}$ Mn at baseline and stimulating glucose concentrations. There was a 150 ms decrease in the average T_1 relaxation time upon introduction of Mn ($p<0.01$). A significant drop from 1362 ms to 861 ms was measured on average after the tissue was activated with $16.7\mu\text{M}$ glucose in presence of $50\mu\text{M}$ Mn ($p<0.0001$). Although this technique is its infancy, *in-vivo* applications have shown very promising results and we anticipate it being an effective tool to assess transplanted islets functional mass as well.

So far there have been very limited reports of T_1 contrast agents used for *in-vivo* MRI of transplanted islets. Both approaches used Gd chelated compounds but in one case it was used as a blood pool agent in dynamic contrast enhanced MRI (DCE MRI) to assess angiogenesis in transplanted islets [35] while the other application used it for *in-vitro* labeling of isolated islets [33]. Islet revascularization is fundamental in maintaining graft viability and proper functionality and lack of blood supply is known to contribute to early graft loss [50-53]. DCE-MRI has been used extensively to monitor developing tumor growth and vasculature. The transplanted islet plug could be considered an analogous system of developing vessels and therefore open to the application of DCE-MRI to observe how changes in vasculature impact β -cell function. Preliminary results have shown that at day 14 post-transplantation, kidney grafts have higher overall Gd-DTPA concentration and that its peak concentration is achieved significantly faster than at day 3 indicating a more developed microvascular network [35]. However, this study did not directly relate DCEMRI parameters to morphologic and morphometric data. In Biancone *et al.*, 2007 [33] GdHPD03A was used as an *in-vitro* labeling agent for both mouse

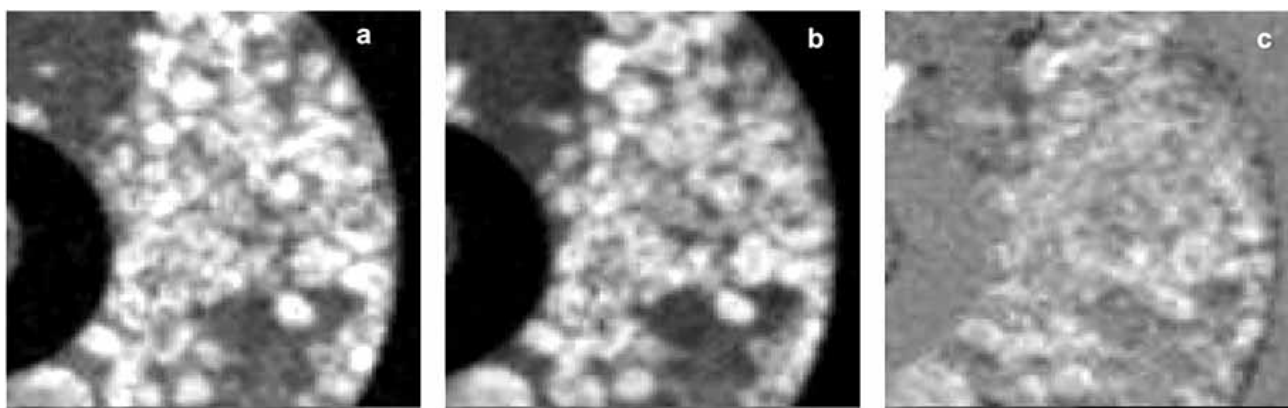


Fig. (1). Manganese induced MRI signal enhancement in perfused isolated human islets. a) Spin echo image of human islets in a MR perfusion chamber following perfusion with Krebs-Ringer Buffer supplemented with 2mM glucose and 50µM MnCl₂; b) following perfusion with Krebs-Ringer Buffer supplemented with 16mM glucose and 50µM MnCl₂; c) subtraction image (b-a) showing showing signal enhancement due to glucose activation induced Mn uptake. Acquisition parameters: TR/TE = 400/7.8 ms, matrix = 128x128, FOV = 0.45 cm, slice thickness = 0.3 mm, in-plane resolution = 40 µm, NEX = 20. Temperature= 35°C.

and human isolated islets used in a rodent kidney transplant model. T₁ weighted images showed an initial increase in signal intensity during the first 10 days post-transplantation which was attributed to intracellular redistribution of Gd. However, considering that a significant loss of viable islets occur within the first few days post-transplant even in syngeneic and immunocompromised recipients, this increase in signal is also likely due to Gd being released in the extracellular milieu by apoptotic islets and therefore a correlation between changes in signal and remaining viable islets in the kidney graft seems problematic at this time.

Presently, iron particles are the main contrast agent used for MRI studies of transplanted islets. The first study by Jirak and others used commercially available SPIO in a rat model of intrahepatically transplanted islets and showed non-homogeneous hypointense regions in T₂^{*}-weighted images at 4.7T for up to 22 weeks after transplantation, however no quantitative measurements of signal changes were performed [19]. Similar results were shown by Evgenov *et al.*, 2006 in a kidney and liver transplant model in nude mice at 4.7 T [28]. Modified iron particles carrying a near-infrared fluorescent reporters allowed for both optical and MRI imaging *in-vitro* as well as *in-vivo*. While *in-vivo* data of the kidney capsule transplant showed stable T₂^{*} values up to 188 days, intraportally infused islets were characterized by an initial increase in T₂^{*} values during the first 3-4 days post-transplantation and were stable up to day 7, the last day of MRI examination (Fig. 2). More extensive studies on the clinically relevant model of intrahepatic transplantation were carried out by the same group using commercially available and FDA approved ferumoxide nanoparticles [54]. Iron-labeled human islets were infused in both immunocompromised *Nod.scid* and immunocompetent Balb/c healthy mice. Quantitative analysis of relative islet loss were performed at 4.7T with T₂^{*} weighted images covering the entire liver. Data showed a significant correlation between loss of signal voids in MR images and the rate of islet death obtained from histological data due to immunorejection and non-immune related events thereby confirming MRI as a feasible technique for *in-vivo* tracking of transplanted islets. A similar study carried out in rats confirmed the previous findings with regard to allogeneic islets transplanted in immunocompetent animals and showed a 65% loss of the initial transplanted mass over a period of 6 weeks post-transplantation [55]. However, their immunocompromised model showed only a non significant islet loss at the end of the 6 weeks which would not reflect the early loss of islets due to poor engraftment resulting from damages sustained during the isolation procedure, to ischemia injury and non specific inflammation events occurring in the liver microenvironment [18, 56-58]. Most of these studies were carried

out in healthy non-diabetic animals and therefore did not take into account physiologic changes due to diabetes, particularly the toxic effect of sustained high glucose concentrations on pancreatic islets. In fact, iron labeled islets transplanted intrahepatically in diabetic animals showed a markedly higher apoptotic rate than healthy animals, which could still be successfully detected in T₂^{*} MR images [59].

Clinically relevant studies however have to take into consideration the use of lower field clinical MRI magnets, typically 1.5T or 3T, and their lower spatial resolution which together reduce the sensitivity to SPIO particles. Tai and others, 2006 first reported imaging iron tagged islets at 1.5T [60]. As little as 200 syngeneic islets grafted under the kidney capsule were successfully detected in healthy rats as shown in Fig. 3. Although relevant, in this model transplanted islets are clustered together forming a large pool of iron that produces the so called "blooming artifact" resulting in a signal void larger than the actual area occupied by the iron labeled cells and therefore not amenable to quantitation. As showed *in vitro*, this problem could be addressed by the implementation of new pulse sequences that suppress the blooming artifact while maintaining sensitivity to the magnetic susceptibility of iron [61] and by selectively labeling only a representative fraction of the transplanted islets.

As we look further into the clinical translation of this technique, studies in larger animal models are needed to better mimic the more complex physiology of actual patients and to devise better analytical methods considering the much larger number of islets transplanted and consequently of ROIs in MR images: several hundred thousands in human transplant recipients compared to a few hundred in animals. An initial study was conducted in healthy pigs infused intrahepatically with magnetoencapsulated human islets [62]. Islets were indirectly labeled by dispersing SPIO particles within the alginate coating. T₂^{*}-weighted images acquired on a 1.5T clinical scanner up to 4 weeks post-transplantation revealed the presence of hypointense regions mainly located in the distal vasculature throughout the liver confirming the ability to non-invasively follow delivery and engraftment of pancreatic islets via MRI as shown in Fig. 4. Although no quantitation was performed of the magnetocapsules or islet mass, the authors merged two very interesting techniques: encapsulation and MRI cell tracking. They also explored the use of the inversion-recovery on-resonance (IRON) positive contrast pulse sequence which converts hypointense iron induced voids into hyperintense objects and could facilitate the identification and computation of changes in islet mass [63]. Recent modifications to the encapsulation material were proposed with the addition of gold nanoparticles to provide X-ray

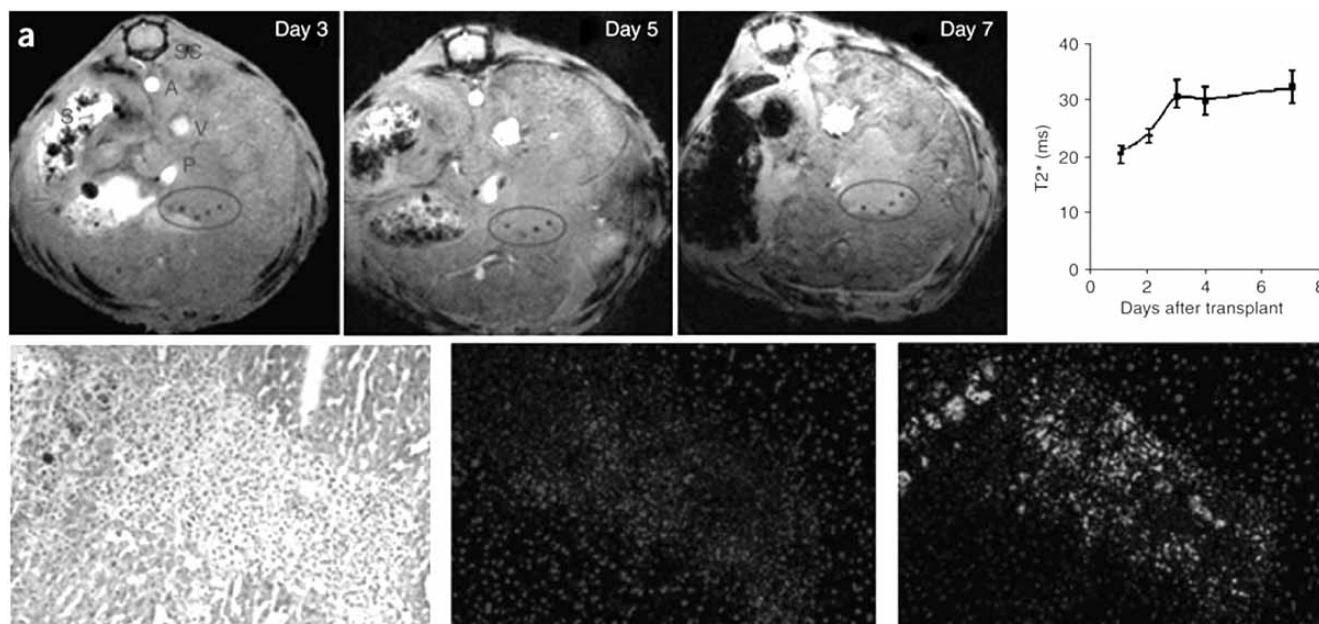


Fig. (2). *In vivo* MRI of intrahepatic transplantation of labeled human islets in streptozotocin-induced diabetic mice. (a) A representative slice (0.5 mm) showing islets scattered throughout the liver. Pancreatic islets appear as hypointense spots on T2^{*}-weighted images (red ovals). S, stomach; SC, spinal cord; P, portal vein; A, aorta; V, caudal vena cava. The graph shows T2^{*} values during the initial post-transplantation period. (b) Correlative microscopy of a frozen liver section. Left, H&E stain showing pancreatic islet within the liver tissue; middle and right, fluorescence microscopy. Cy5.5 signal from MN-NIRF probe (red, middle) is associated with the islet as well as FITC signal (green, left) indicating staining for insulin. Evgenov *et al.* Nat Med 2006; 12(1): 144-8 [28].

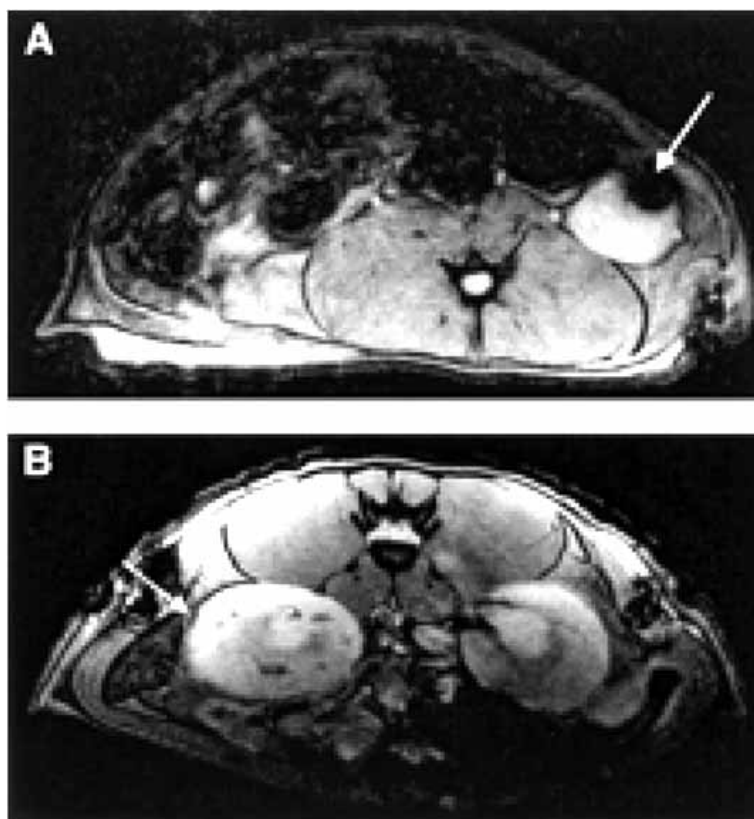


Fig. (3). *In vivo* T2^{*}-weighted gradient echo image. **a)** Lewis rat transplanted with SPIO-labeled 2,000 islet isografts under kidney capsules. The very high iron concentration in this region leads to a large blooming artifact in these gradient echo images (arrow). **b)** Lewis rat transplanted with 200 SPIO-labeled islet isografts in the kidney subcapsular area, showing the black signal void of SPIO-labeled islets surrounded by the capsule (arrow). Tai *et al.* Diabetes 2006; 55: 2931-8 [60].

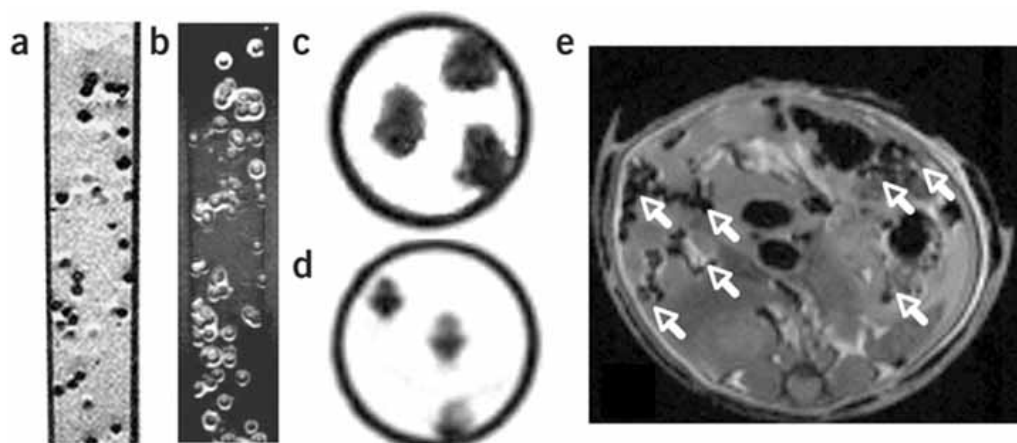


Fig. (4). MRI appearance of magnetocapsules. As magnetocapsules rapidly settle in solution, they were embedded in a 2% agarose phantom at a density of 50 capsules per ml of gel. By using conventional T_2^* -weighted images (a), individual magnetocapsules can be easily identified as hypointensities. By using the IRON sequence for generating positive contrast (b), individual magnetocapsules appear as a bright signal with depiction of the capsule surface. (c,d) Magnetocapsules before (c) and after (d) rupture using glass bead treatment. After rupture, a considerable loss of hypointensity occurs and the Feridex-induced contrast decreases to a pinpoint double-dipole T_2^* susceptibility effect. (e) Magnetic resonance image of a mouse after injection of 500 magnetocapsules in the peritoneal cavity. Single capsules are easily identified (arrows). Barnett *et al.* Nat Med 2007; 13: 986-91 [62].

opacity and ultrasound reflection or the replacement of iron nanoparticles with Gd chelated gold nanoparticles to provide in this case positive MRI contrast [64]. Both these devices would allow for multimodal monitoring of capsule distribution and showed promising, albeit preliminary results, in a mouse model. To reduce the bias given by subjective manual evaluation Jirak and others developed an automated segmentation method which was applied to 3D high resolution data sets and takes into account signal voids present in all slices to determine the total volume of signal loss corresponding to iron labeled islets [65]. The quantitation is still relative as changes in signal loss are normalized to the total volume measured on day one post-transplantation. The need for high resolution, high signal-to-noise ratio images may also limit the applicability to clinical data sets but certainly it allows for faster, more reproducible and objective analysis. *In-vivo* imaging of autologous islet grafts in a pre-clinical non-human primate animal model was recently reported [57]. In this study as well the iron labeled islets were quantified via a semiautomated computational method which uses automated segmentation to classify the ROIs based on their T_2^* values. The data, represented as the number of voxels occupied by the graft as a function of time, confirmed the applicability of iron-labeling for the non-invasive, longitudinal detection of pancreatic islets. However, the quantitation was again relative to the data acquired on the first day post-transplantation and attempts to relate this data to the absolute number of islets were not reported and while the number of voxels in the liver grafts decreased over time as expected, the kidney transplant registered a constant increase of voxels which was not explained (Fig. 5). The first clinical study also was able to show safety and feasibility of the technique by monitoring four islet transplant patients up to six months post-transplantation [18]. ROI analysis was performed manually and no correlation was found between signal voids in the liver and the number of transplanted islets. Moreover in two cases, iron overload in the liver caused a strong enough background signal that completely impaired image analysis. These results reiterate the importance of having not only a non-invasive imaging technology for repeated serial monitoring of transplanted pancreatic islets, but one that allows for the actual quantitation of the islet mass and, ideally, islet function.

MRI OF ENDOGENOUS PANCREATIC ISLETS

Despite tremendous progress, non-invasive *in-vivo* imaging of pancreatic islets remains a daunting challenge. Changes in both islet mass and function have been long associated with the onset of

diabetes but exact details are still unknown. The temporal evolution of the disease with respect to these changes remains unknown and several fundamental questions are still unanswered. For example, it is still not clear whether the loss of pancreatic islet mass precedes and precipitates the onset of diabetes, and whether changes in mass and function progress simultaneously and equally affect individual islets [66]. Moreover, early detection of the pathology would greatly enhance the result of approaches aiming at maintaining or possibly restoring islet function.

All the current knowledge on human β -cell mass *in-vivo* has been derived by morphometric analysis in pancreas obtained at autopsy [2-5, 67]. Indirect estimates are routinely carried out *in-vivo* by measuring insulin secretion and C-peptide levels during oral glucose or meal challenges. However the great variability in islet mass among different individuals contributes to the difficult data interpretation. Longitudinal studies in human subject would greatly enhance our knowledge and bring us closer to the development of effective therapies.

It is likely that different non-invasive techniques will be applied in a multimodal approach involving among others PET, CT, and MRI but, as previously mentioned, thus far even *in-vivo* studies of endogenous pancreatic islet mass and function in animal models are quite limited. Most of the published literature focuses on imaging insulinitis, the autoimmune inflammation process leading to the onset of type I diabetes, by labeling T-cells with iron particles. The first of such studies utilized SPIOs cross-linked with the membrane translocation signal of the HIV-1-Tat protein to promote intracellular uptake [68]. Lymphocytes isolated from diabetic NOD mice were labeled and infused in NOD.scid which are unable to develop diabetes due to immature lymphocytes. Their pancreas was excised 24 hours later and imaged both via fluorescence microscopy and MRI at 14.1T and 1.5T. Images clearly showed major infiltration in correspondence of pancreatic islets and demonstrated the potential to directly visualize insulinitis. Moore then proceeded to develop very interesting iron nanoparticles which were cross-linked with avidin-fluorescein isothiocyanate for FACS sorting, with ^{125}I to allow for quantitation and finally with NRP-V7, a peptide that binds specifically to a subpopulation of CD8^+ T-cells which are diabetogenic in NOD mice [21]. Again, an adoptive transfer model was used and the recruitment of autoreactive T-cells to the pancreas *in-vivo* over a period of 16 days after the transfer was clearly visualized *in-vivo*. Similar results were achieved in an analogous animal model using anionic magnetic nanoparticles (AMNPs) [69].

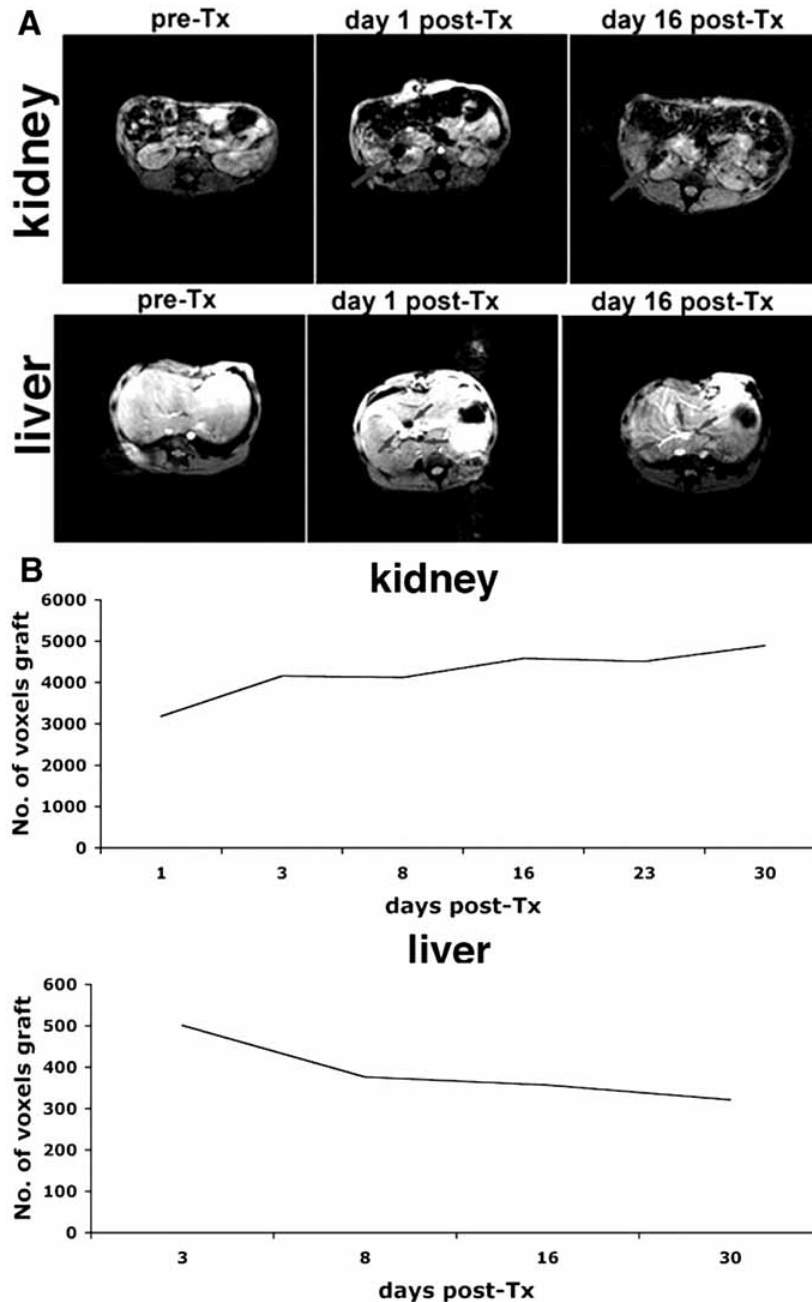


Fig. (5). Longitudinal magnetic resonance imaging (MRI) of labeled autologous islets transplanted into the right renal capsule (top) and the liver (bottom) of a baboon (animal B173). (A) pretransplant images of the liver and kidney do not show signal voids, representative of labeled islets. The right renal islet graft site appears as a large pocket of signal loss. Arrows point to the graft. In the liver, MRI reveals distinct foci of signal loss, corresponding to labeled islets along the vascular branches. (B) Semiquantitative assessment of graft longevity indicates relative graft stability more than 16 days after transplantation. (A) pretransplant images of the liver and kidney do not show signal voids, representative of labeled islets. The right renal islet graft site appears as a large pocket of signal loss. Arrows point to the graft. In the liver, MRI reveals distinct foci of signal loss, corresponding to labeled islets along the vascular branches. (B) Semiquantitative assessment of graft longevity indicates relative graft stability more than 16 days after transplantation. Medarova *et al.* Transplantation 2009; 87: 1659-66 [57].

The advantage of these particles is the strong effect on protons which facilitates *in vivo* studies in clinical conditions and their negative surface charges which provide high cell uptake even after one hour of incubation.

None of the studies presented however could prove that individual cells can be detected via MRI, nor was any quantitation was carried out, due to the difficulties associated with SPIOs previously described. However, Moore and her group recently

advanced the significance of their studies by infusing the MN-NRP-V7 particles systemically in wild type NOD mice of different ages and were able to image *in vivo* at 9.4T the spontaneous recruitment and accumulation of native IGRP₂₀₆₋₂₁₄-reactive CD8⁺ T lymphocytes at different stages of diabetes progression [70]. The degree of infiltration was measured as percentage of change in T₂ relaxation time and reached the peak in 8 weeks old animals to then taper off. MRI data was confirmed by FACS analysis of both circulating and

intra-islet T-lymphocytes with the most MN-NRP-V7 reactive ones found again in 8 weeks old animals. Reactivity levels quickly dropped in 15 and 24 week old mice as shown in Fig. 6. This is a very relevant study as for the first time the evolution of an antigen-specific immunity in Type I diabetes was followed non-invasively *in-vivo*. It also shows the possible clinical translation of this technique although the sensitivity of clinical magnets to the amount of iron accumulated in the pancreas during the inflammation process remains to be seen. PFPE nanoparticles seem to overcome most of these limitations, as shown by Srinivas *et al.* [31] who were able to visualize and quantify *in vivo* T-cell infiltration using spin density-weighted ^{19}F MRI. Similarly to the studies above, T-cells were isolated from BDC2.5 TCR transgenic mice, activated and labeled with PFPE before being transferred intraperitoneally into cyclophosphamide (CPA) treated NOD.scid mice. Animals were imaged 48 hours later to allow for T-cell homing. Proton density MR images were used as anatomical reference for ^{19}F images which selectively show the signal coming from labeled cells. The quantity of apparent PFPE-labeled cells was calculated using external ^{19}F references and was confirmed by MR imaging of the isolated pancreas as well as by optical imaging and histology. Results showed that 48 hours after injection, about $2.2 \pm 0.9\%$ of the transferred cells had infiltrated the pancreas. Only one time point was considered here but a similar study reported successfully imaging ^{19}F labeled lymphocytes over 21 days [32] and although factors such as cell division and cell death may potentially affect the accuracy of the quantification, ^{19}F MRI certainly seems very promising and could be easily applied to the monitoring of transplanted pancreatic islets.

A different approach to MR pancreatic islet imaging has recently been proposed which exploits modifications in islet vasculature associated with different pathological conditions. While comprising 1-2% of the pancreas the endocrine tissue receives up to 15% of the whole organ's blood supply [71]. Its capillary network is five times richer than that of the exocrine tissue and each islet has a glomerulus like vascular structure with ten times more fenestrae than exocrine tissue capillaries [14, 72]. Streptozotocin induced diabetic animals have been shown to undergo increase in vascular permeability and islet blood flow and volume as early as few hours after the treatment and before the onset of diabetes symptoms [63, 73-75]. Similarly, infiltration of leucocytes around and into pancreatic islets has been found to cause disruption of the vasculature resulting in leaky capillaries [76-78]. Therefore progression of insulinitis could be monitored by measuring the leakage of the microvasculature surrounding and within pancreatic islets. This has been done recently by several groups employing mostly modified SPIOs or chelated Gd complexes. Among the iron based contrast agents considered, CMFN showed good results [61]. CMFN are long circulating magnetofluorescent nanoparticles crosslinked to the Alexa-488 fluorochrome and allow for both fluorescence analysis as well as MR imaging. CMFN particles were injected into BDC2.5/NOD and age matched control from 2 weeks until about 15 weeks. Confocal microscopy and histology confirmed the presence of extravasated CMFN particles mostly surrounding pancreatic islets and in surrounding cells identified as macrophages or dendritic cells. The fluorescent signal measured *in vitro* from excised pancreas was found to match the changes in T_2 relaxation time measured *in vivo* using a 8.5 T animal magnet and showed the inflammation to start around 2-3 weeks of age followed by a decrease and stabilization around 4-6 weeks. The same protocol was repeated with non-fluorescent SPIOs in the same mice treated with CPA to induce 100% penetrance of diabetes and in the more clinically relevant wt NOD mouse [79]. Once again, T_2 values decreased in the BDC2.5/NOD mice after SPIO injection when inflammation was present but returned to normal once the edema had resolved (Fig. 7). Because of the significant individual-to-individual variation in disease progression found in the NOD mice, T_2 values

measured in the pancreas ranged from normal to diabetic in age matched animals according to the stage of insulinitis. They also found a correlation between MRI parameters and response to anti CD3 mAbs, an immunotherapy which can reverse recent onset diabetes and restore self tolerance, starting at day 3 after completion of anti-CD3 treatment. All together, these data confirmed that pancreatic inflammation can be successfully monitored by SPIO-MRI. However the authors found that values measured at 13 and 20 weeks were not predictive of the time at which diabetes was eventually diagnosed and therefore concluded that this technique is unlikely to help assess an individual's long-term risk of developing autoimmune diabetes.

Assessment of the vasculature in the studies described above was performed by histology but the use of a nanosized protected graft copolymer (PGC) covalently linked to GdDTPA labeled with fluorescein isothiocyanate (FITC) allowed for both MRI analysis and 3D angiographic imaging [34]. Changes in the vasculature of STZ BALB/c mice for up to 40 hours after administration of the contrast agent were detected by measuring T_1 changes and were compared with the whole-body vascular distribution of PGC-GdDTPA-F (Fig. 8). Significant differences were seen at 1 and 17 hours post injection but at 40 hours the agent was cleared from the pancreas and therefore longitudinal monitoring of the inflammation would require repeated administration. Also, different time points were not considered so it was not clear whether this technique could discriminate between different stages of the disease.

Despite DCEMRI sensitivity to microvasculature, surprisingly, to the best of our knowledge, a very limited number of clinical studies have applied it to the pancreas and only in one case was it used to investigate changes in pancreatic tissue perfusion due to chronic pancreatitis [80, 81]. Traditionally these studies use Gd chelates as reporters or vasculature permeability. In order to better link beta cell functionality to vasculature morphology our group has recently performed DCEMRI studies using Mn as a functional T_1 relaxation agent to not only detect changes in pancreatic islet microvasculature but also acquire islet functional information based on the fact that signal intensities depend on both the uptake and accumulation of Mn in the targeted tissue [45]. In STZ induced diabetic mice the decrease in beta cell mass associated with diabetes resulted in a rapid Mn washout from the pancreas not evident in healthy control animals. Supporting these data were a longer time to peak enhancement and continuous increase in signal in the control pancreas due to delivery and accumulation of Mn in these cells.

All the approaches presented so far have not directly imaged pancreatic islets mass or function, rather have exploited the pathophysiological changes that the islets and pancreas undergo during the development of diabetes to make an assessment of the inflammation process and indirectly of the islets. The first proof to our knowledge that MRI can directly image islet function *in-vivo* was obtained by our group [46, 82] and is illustrated in Fig. 9. Fasted Lewis rats were first infused with Mn via tail vein and then given an IP glucose bolus. Baseline MR images of the pancreas prior and post Mn administration were acquired and compared with images obtained following pancreatic islet glucose stimulation. Experiments were performed at 4.7T and an inversion recovery MPRAGE sequence was used to enhance Mn induced contrast. Consistent with our *in-vitro* data and with the known affinity of Mn for the pancreas [83], overall increase in signal was seen in the pancreas within minutes from Mn infusion. However, a further significant increase was measured following beta cell activation that was not homogenous throughout the pancreas but rather spatially confined to hot spots dispersed within the pancreatic tissue and similar in size to an islet or islet clusters. Mn concentration in the pancreas was quantified by atomic absorption and showed the same pattern increasing significantly after glucose stimulation.

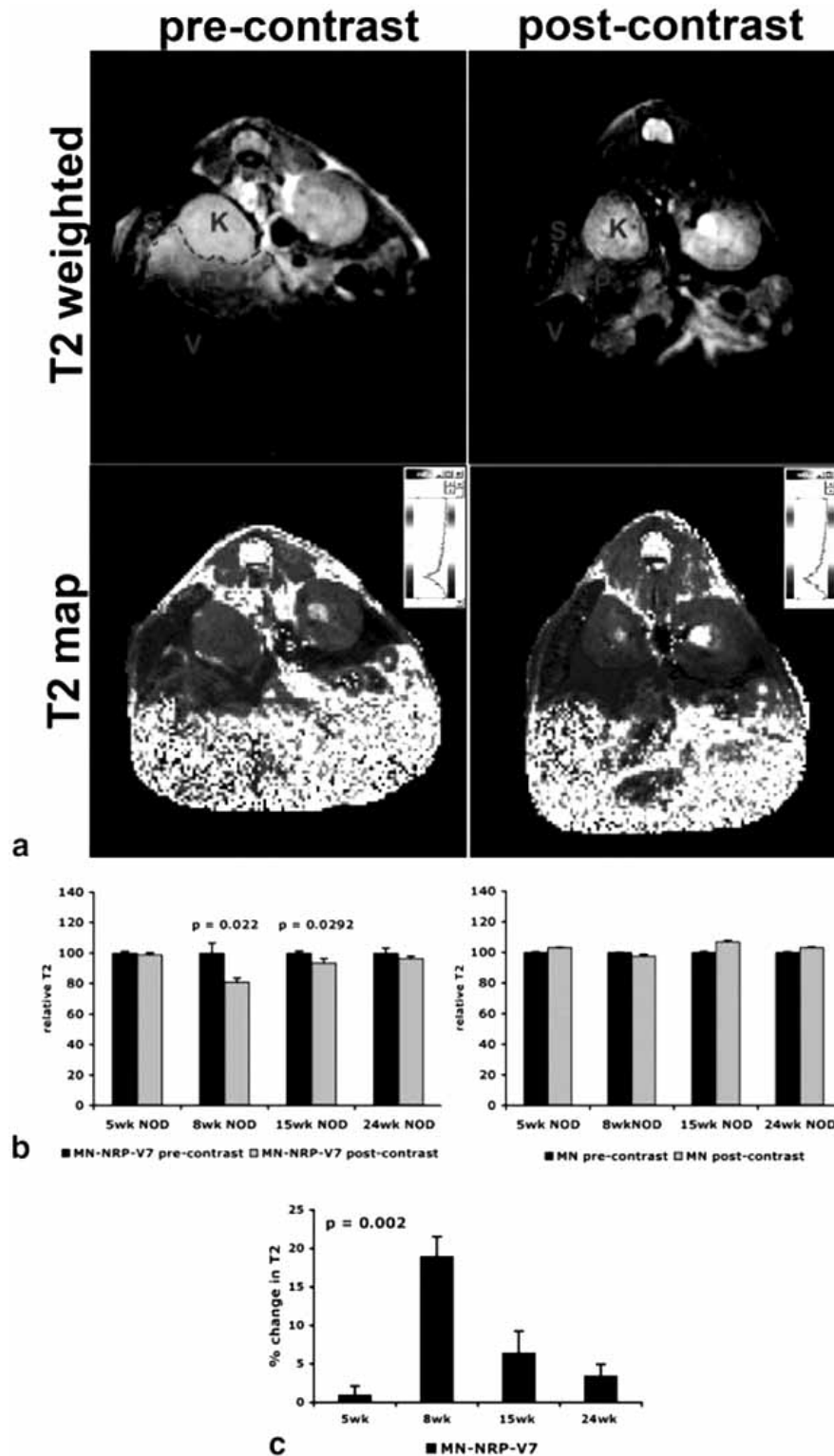


Fig. (6). MRI of NRP-V7-specific CD8+ T lymphocyte infiltration of the pancreas. **a**) A representative T_2 -weighted image (top) and its corresponding multiecho T_2 map (bottom) before (left) and 24 h after (right) intravenous injection of MN-NRP-V7. The pancreas is outlined in red. V = stomach, S = spleen, K = kidney, P = pancreas. **b**) Quantitative representation of the change in T_2 relaxation times (T_2 , ms) as a function of age in 5- ($N = 7$), 8- ($N = 4$), 15- ($N = 4$), and 24-week-old ($N = 10$) NOD mice injected with MN-NRP-V7 (left) or unmodified MN nanoparticles (right). In animals injected with MN-NRP-V7, there was a significant change in T_2 relaxation times after injection at 8 ($P = 0.022$) and 15 ($P = 0.0292$) weeks of age. By contrast, in animals injected with unmodified MN nanoparticles, there was no significant change in T_2 values. Data (mean \pm SEM) were analyzed by two-tailed Student's t -test. **c**) The change in T_2 in animals injected with MN-NRP-V7 followed a trend of age dependence, with a peak at 8 weeks of age. Data (mean \pm SEM) were analyzed by one-way ANOVA with Tukey's post-hoc pairwise comparison test. $**P = 0.002$. Medarova *et al.* Mag Res Med 2008; 59: 712-20 [70].

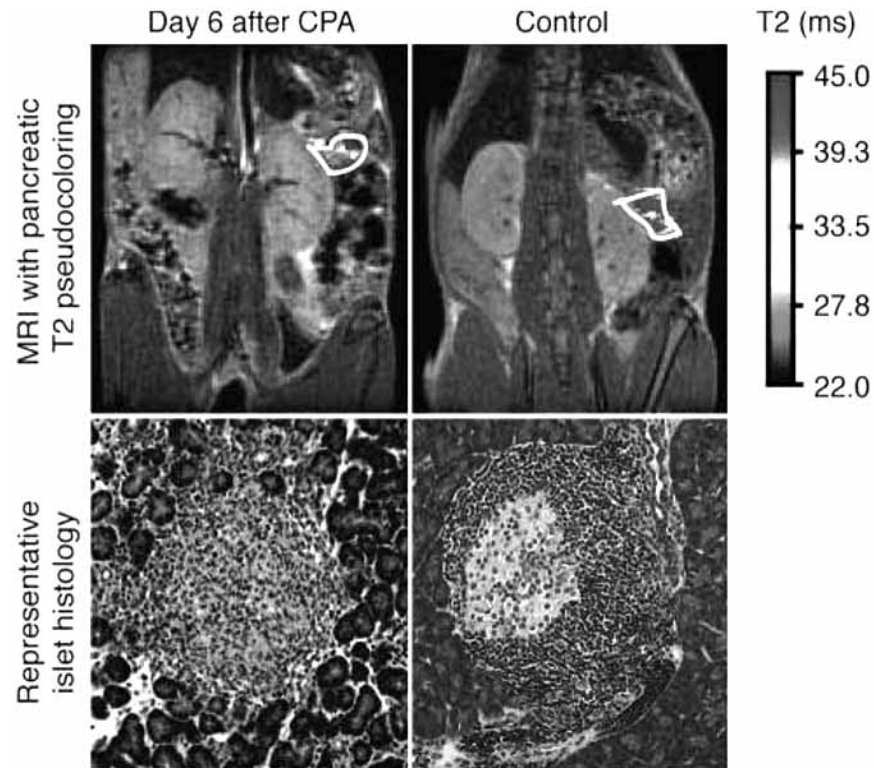


Fig. (7). Severity of insulitis revealed by noninvasive MNP-MRI. Young female BDC2.5/NOD mice were imaged on day 6 after CPA treatment and 24 hours after MNP injection. Outlined regions correspond to the pancreas and in the original figure were pseudocolored to reflect the T_2 value of the organ (approximately 25 ms and 40 ms for the CPA treated and control group respectively). Photomicrographs show representative islet histology from these animals. Magnification, $\times 20$. Turvey *et al.* *J Clin Invest* 2005; 115: 2454-61 [79].

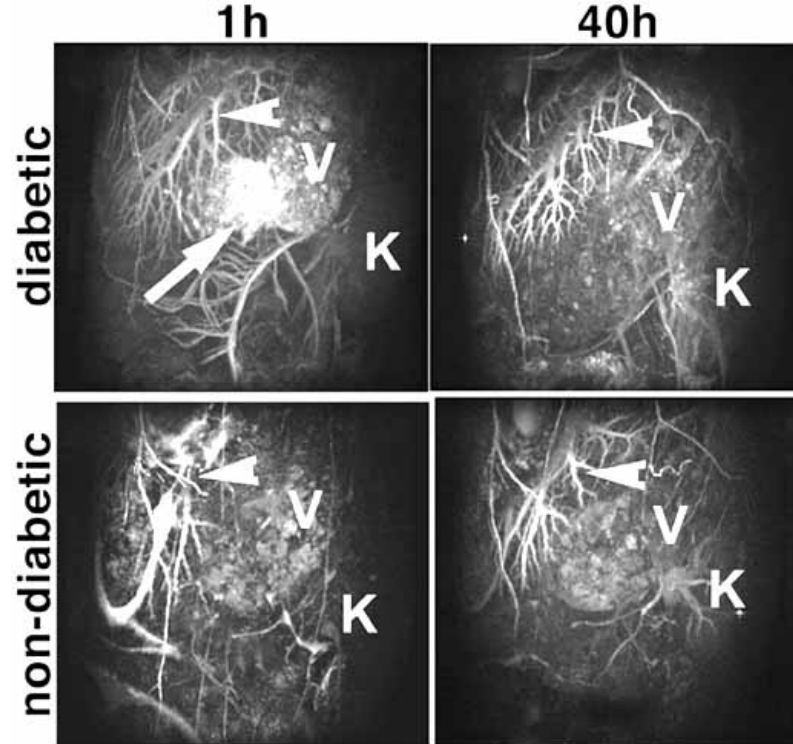


Fig. (8). High-resolution 3D MR angiography of STZ-induced diabetic mice and nondiabetic controls obtained 1 and 40 h after injection of PGC-GdDTPA-F. The hepatic vasculature is outlined following injection of the contrast agent (arrowheads). In diabetic animals, the pancreas is associated with bright diffuse enhancement at 1 h postinjection (arrow), consistent with increased vascular volume and leakage into the interstitium. This is followed by a washout by 40 h. Nondiabetic animals showed no enhancement in the area of the pancreas. K, kidney; V, stomach. Medarova *et al.* *Diabetes* 2007; 56: 2677-82 [34].

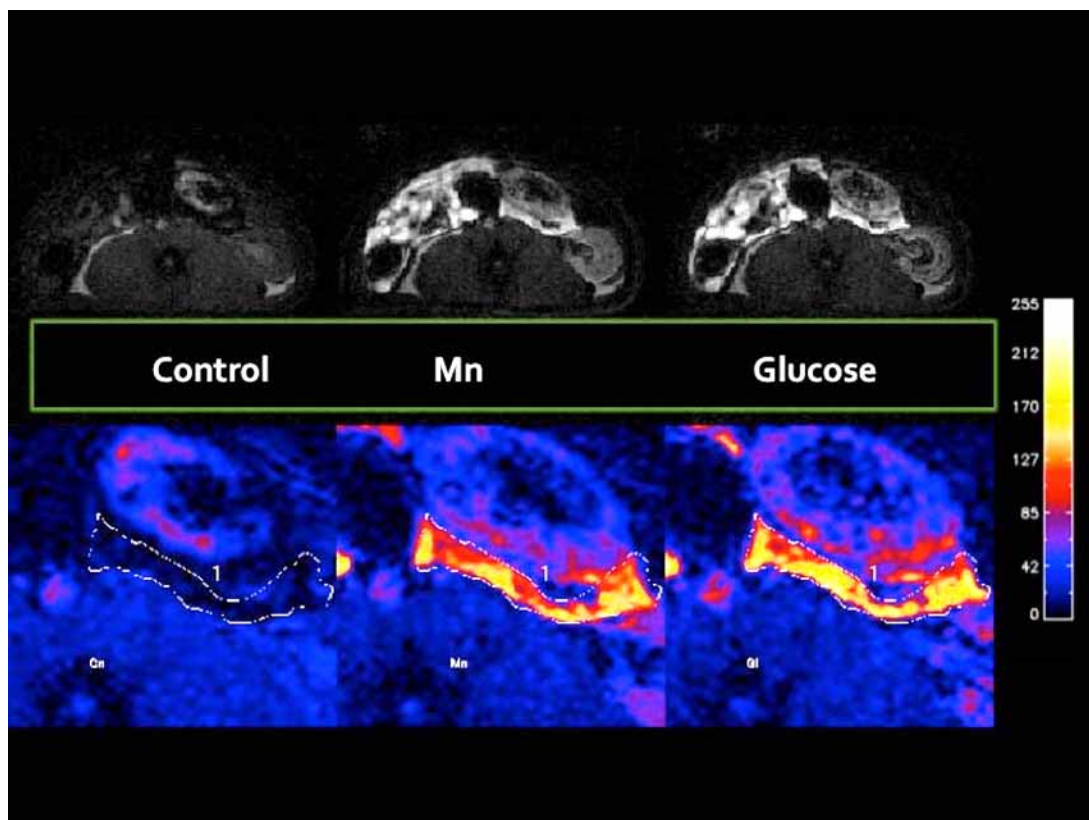


Fig. (9). *In vivo* functional Mn enhanced MRI (MEMRI) of glucose activated pancreas. Axial images of Lewis rat illustrating pancreatic enhancement due to manganese infusion followed by glucose activation. Top Row: Passive Mn uptake is clearly seen in the pancreas as well as in surrounding organs following Mn infusion. Glucose activation stimulates further Mn uptake in the pancreas. Bottom Row: Pancreatic region of interested is indicated by the white dotted line in the pre-Mn image. The color bar maps the color with image signal and indicates the changes in image contrast due to Mn accumulation. Glucose activated Mn uptake occurs throughout the pancreas and translates into a 10-35% increase in image contrast. This enhancement pattern is not found in STZ induced diabetic animals. Mn Dose: 26 nmol/g bw, Glucose: 0.75g/kg. MPRAGE: TE = 2.93ms, echo TR = 9.72ms, FA = 10, Segment TR = 2.5s, IT = 750ms, NEX = 4, Matrix = 160 x 160, FOV = 6.0 x 5.50 cm. Haque ME, *et al.* Proceedings of the 17th Annual Meeting of ISMRM, Honolulu, Hawaii, USA 2009 [82].

Notably, the tail of the pancreas that corresponds to the splenic region analyzed in the MR images, was found to have the highest increase in Mn concentration.

Control STZ induced diabetic animals only had non-specific Mn uptake which was not enhanced by glucose. Similar conclusions were achieved *in-vivo* using a mouse model [47]. Data analysis in this study was based on a single slice per pancreas and therefore limited to a small portion of the whole pancreas. Improved analytical methods are needed in order to identify larger portions of the pancreas with certainty and to automatically compute signal enhancement without the bias that hand selected ROIs can introduce.

Similar results were recently reported by Antkowiak *et al.* [47] although their experimental approach varied. Unlike our study where signal changes due to passive and active Mn uptake were quantified in the same animal, here a control group received IV saline and IP Mn while the activated group was administered glucose first followed by IP Mn. A 50% increase in the normalized pancreas signal was measured in the glucose-activated group which was not seen in STZ induced diabetic animals. Given that only one slice per animal was analyzed, that the signal was averaged over the entire area and that islets represent 1-2% of the pancreas, the magnitude of the signal increase reported seems disproportionate and possibly includes the enhancement caused by increased glucose metabolism. Also, Mn uptake due to first phase insulin secretion, which represents β -cells strongest activation, was only partially

accounted as the contrast agent was injected 2 minutes after glucose administration. Nonetheless, the potential of using Mn as an *in-vivo* reporter of β -cell function was confirmed. In general, a more accurate interpretation of Mn effect on MR signal enhancement will come from a deeper understanding of its intracellular handling as well as from better image analysis methods.

CONCLUSIONS

Despite recent progress, noninvasive imaging of pancreatic islet mass and function remains a challenging task. Due to its noninvasive nature, to excellent soft tissue contrast, high spatial resolution, and to the continuous development of beta cell specific contrast agents MRI has quickly become a powerful tool in the investigation of beta cell mass and function and their dynamic changes over time. The availability of both high field narrow bore and animal systems provide investigators with the ability to study islets in a continuum from isolation, transplantation, and even rejection. With the continued maturation of these techniques and careful understanding of the sources of MR contrast in the pancreatic islet, MRI can help in the understanding of how islets function independently, and as functional syncytium as in the endogenous pancreas. It is through this understanding that the pathology of diabetes and pancreatic cancer may also be further understood. It is also critical to the advancement of MRI that we continue to use and learn from other imaging modalities which provide critical information on islet function.

ACKNOWLEDGEMENTS

This work was financially supported in part by NIH R01001828 and NIDDK/BCBC to BBR. We thank the ICR Basic Science Islet Distribution Program for providing the islets used in these studies.

REFERENCES

References 84-86 are related articles recently published.

- [1] Truong W, Lakey JR, Ryan EA, Shapiro AM. Clinical islet transplantation at the University of Alberta--the Edmonton experience. *Clin Transpl* 2005; 153-72.
- [2] Matveyenko AV, Butler PC. Relationship between beta-cell mass and diabetes onset. *Diabetes Obes Metab* 2008; 10 (Suppl 4): 23-31.
- [3] Junker K, Egeberg J, Kromann H, Nerup J. An autopsy study of the islets of Langerhans in acute-onset juvenile diabetes mellitus. *Acta Pathol Microbiol Scand A* 1977; 85(5): 699-706.
- [4] Butler AE, Galasso R, Meier JJ, Basu R, Rizza RA, Butler PC. Modestly increased β -cell apoptosis but no increased β -cell replication in recent-onset type 1 diabetic patients who died of diabetic ketoacidosis. *Diabetologia* 2007; 50(11): 2323-31.
- [5] Kloppel G, Drenck CR, Oberholzer M, Heitz PU. Morphometric evidence for a striking β -cell reduction at the clinical onset of type 1 diabetes. *Virchows Arch A Pathol Anat Histopathol* 1984; 403(4): 441-52.
- [6] Eckhard M, Brandhorst D, Winter D, Jaeger C, Jahr H, Bretzel RG, *et al.* The role of current product release criteria for identification of human islet preparations suitable for clinical transplantation. *Transplant Proc* 2004; 36(5): 1528-31.
- [7] Medarova Z, Moore A. MRI as a tool to monitor islet transplantation. *Nat Rev Endocrinol* 2009; 5(8): 444-52.
- [8] Medarova Z, Moore A. MRI in diabetes: first results. *AJR Am J Roentgenol* 2009; 193(2): 295-303.
- [9] Gaglia JL. Noninvasive imaging of islet transplantation and rejection. *Curr Diabetes Rep* 2007; 7(4): 309-13.
- [10] Malaisse WJ, Louchami K, Sener A. Noninvasive imaging of pancreatic beta cells. *Nat Rev Endocrinol* 2009; 5(7): 394-400.
- [11] Medarova Z, Moore A. Non-invasive detection of transplanted pancreatic islets. *Diabetes Obes Metab* 2008; 10 (Suppl 4): 88-97.
- [12] Virostko J, Jansen ED, Powers AC. Current status of imaging pancreatic islets. *Curr Diabetes Rep* 2006; 6(4): 328-32.
- [13] Souza F, Freeby M, Hultman K, Simpson N, Herron A, Witkowsky P, *et al.* Current progress in non-invasive imaging of β -cell mass of the endocrine pancreas. *Curr Med Chem* 2006; 13(23): 2761-73.
- [14] Bonner-Weir S, Orci L. New perspectives on the microvasculature of the islets of Langerhans in the rat. *Diabetes* 1982; 31(10): 883-9.
- [15] Buchwald P, Wang X, Khan A, Bernal A, Fraker C, Inverardi L, *et al.* Quantitative assessment of islet cell products: estimating the accuracy of the existing protocol and accounting for islet size distribution. *Cell Transplant* 2009; 18(10): 1223-35.
- [16] Kaihoh T, Masuda T, Sasano N, Takahashi T. The size and number of Langerhans islets correlated with their endocrine function: a morphometry on immunostained serial sections of adult human pancreases. *Tohoku J Exp Med* 1986; 149(1): 1-10.
- [17] Tons HA, Terpstra OT, Bouwman E. Heterogeneity of human pancreata in perspective of the isolation of the islets of langerhans. *Transplant Proc* 2008; 40(2): 367-9.
- [18] Toso C, Vallee JP, Morel P, Ris F, Demuylder-Mischler S, Lepetit-Coiffe M, *et al.* Clinical magnetic resonance imaging of pancreatic islet grafts after iron nanoparticle labeling. *Am J Transplant* 2008; 8(3): 701-6.
- [19] Jirak D, Kriz J, Herynek V, Andersson B, Girman P, Burian M, *et al.* MRI of transplanted pancreatic islets. *Magn Reson Med* 2004; 52(6): 1228-33.
- [20] Raynal I, Prigent P, Peyramaure S, Najid A, Rebuzzi C, Corot C. Macrophage endocytosis of superparamagnetic iron oxide nanoparticles: mechanisms and comparison of ferumoxides and ferumoxtran-10. *Invest Radiol* 2004; 39(1): 56-63.
- [21] Moore A, Grimm J, Han B, Santamaria P. Tracking the recruitment of diabetogenic CD8⁺ T-cells to the pancreas in real time. *Diabetes* 2004; 53(6): 1459-66.
- [22] Rogers WJ, Basu P. Factors regulating macrophage endocytosis of nanoparticles: implications for targeted magnetic resonance plaque imaging. *Atherosclerosis* 2005; 178(1): 67-73.
- [23] von Zur Muhlen C, von Elverfeldt D, Bassler N, Neudorfer I, Steitz B, Petri-Fink A, *et al.* Superparamagnetic iron oxide binding and uptake as imaged by magnetic resonance is mediated by the integrin receptor Mac-1 (CD11b/CD18): implications on imaging of atherosclerotic plaques. *Atherosclerosis* 2007; 193(1): 102-11.
- [24] Riviere C, Wilhelm C, Cousin F, Dupuis V, Gazeau F, Perzynski R. Internal structure of magnetic endosomes. *Eur Phys J E Soft Matter* 2007; 22(1): 1-10.
- [25] Malosio ML, Esposito A, Poletti A, Chiaretti S, Piemonti L, Melzi R, *et al.* Improving the procedure for detection of intrahepatic transplanted islets by magnetic resonance imaging. *Am J Transplant* 2009; 9(10): 2372-82.
- [26] Ris F, Lepetit-Coiffe M, Toso C, Armanet M, Crowe LA, Bosco D, *et al.* Radio-histological correlation and comparative assessment of iron oxide nanoparticles for islet labeling in human islet graft MRI monitoring. In: *Imaging the Pancreatic β -Cell, 4th Workshop*. Washington, DC 2009.
- [27] Evgenov NV, Medarova Z, Pratt J, Pantazopoulos P, Leyting S, Bonner-Weir S, *et al.* *In vivo* imaging of immune rejection in transplanted pancreatic islets. *Diabetes* 2006; 55(9): 2419-28.
- [28] Evgenov NV, Medarova Z, Dai G, Bonner-Weir S, Moore A. *In vivo* imaging of islet transplantation. *Nat Med* 2006; 12(1): 144-8.
- [29] Marzola P, Longoni B, Szilagyi E, Merigo F, Nicolato E, Fiorini S, *et al.* *In vivo* visualization of transplanted pancreatic islets by MRI: comparison between *in vivo*, histological and electron microscopy findings. *Contrast Media Mol Imaging* 2009; 4(3): 135-42.
- [30] Ris F, Crowe LA, Morel P, Armanet M, Masson S, Nielles-Vallespin S, *et al.* Quantification of transplanted iron oxide labeled islet cells using an ultra short echo time acquisition technique at 3T. In: *Imaging the Pancreatic β -Cell, 4th Workshop*. Washington, DC 2009.
- [31] Srinivas M, Morel PA, Ernst LA, Laidlaw DH, Ahrens ET. Fluorine-19 MRI for visualization and quantification of cell migration in a diabetes model. *Magn Reson Med* 2007; 58(4): 725-34.
- [32] Srinivas M, Turner MS, Janjic JM, Morel PA, Laidlaw DH, Ahrens ET. *In vivo* cytometry of antigen-specific t cells using 19F MRI. *Magn Reson Med* 2009; 62(3): 747-53.
- [33] Biancone L, Crich SG, Cantaluppi V, Romanazzi GM, Russo S, Scalabrino E, *et al.* Magnetic resonance imaging of gadolinium-labeled pancreatic islets for experimental transplantation. *NMR Biomed* 2007; 20(1): 40-8.
- [34] Medarova Z, Castillo G, Dai G, Bolotin E, Bogdanov A, Moore A. Noninvasive magnetic resonance imaging of microvascular changes in type 1 diabetes. *Diabetes* 2007; 56(11): 2677-82.
- [35] Hathout E, Sowers L, Wang R, Tan A, Mace J, Peverini R, *et al.* *In vivo* magnetic resonance imaging of vascularization in islet transplantation. *Transplant Int* 2007; 20(12): 1059-65.
- [36] Kohlmeir E, Waters A, Mastarone D, Song Y, Wang L, Kaufman DB, *et al.* Optimizing Tracking of Transplanted Pancreatic Islets With T1 MR Contrast Agents. In: *Imaging the Pancreatic β -Cell, 4th Workshop*. Washington, DC 2009.
- [37] Anguaco TL, Mattison DR, Thomford PJ, Jordan J. Effect of manganese on human placental spin-lattice (T1) and spin-spin (T2) relaxation times. *Physiol Chem Phys Med NMR* 1986; 18(1): 41-8.
- [38] Kang YS, Gore JC. Studies of tissue NMR relaxation enhancement by manganese. Dose and time dependences. *Invest Radiol* 1984; 19(5): 399-407.
- [39] Mamourian AC, Burnett KR, Goldstein EJ, Wolf GL, Kressel HY, Baum S. Proton relaxation enhancement in tissue due to ingested manganese chloride: time course and dose response in the rat. *Physiol Chem Phys Med NMR* 1984; 16(2): 123-8.
- [40] Mendonca-Dias MH, Gaggelli E, Lauterbur PC. Paramagnetic contrast agents in nuclear magnetic resonance medical imaging. *Semin Nucl Med* 1983; 13(4): 364-76.
- [41] Wydrzynski TJ, Marks SB, Schmidt PG, Govindjee, Gutowsky HS. Nuclear magnetic relaxation by the manganese in aqueous suspensions of chloroplasts. *Biochemistry* 1978; 17(11): 2155-62.

- [42] Lauterbur P, Mendonca-Dias M, Rudin A. Augmentation of tissue water proton spin-lattice relaxation rates by *in-vivo* addition of paramagnetic ions. *Frontiers Biol Energy* 1978; 1: 752.
- [43] Hunter DR, Komai H, Haworth RA, Jackson MD, Berkoff HA. Comparison of Ca²⁺, Sr²⁺, and Mn²⁺ fluxes in mitochondria of the perfused rat heart. *Circ Res* 1980; 47(5): 721-7.
- [44] Dryselius S, Grapengiesser E, Hellman B, Gylfe E. Voltage-dependent entry and generation of slow Ca²⁺ oscillations in glucose-stimulated pancreatic β -cells. *Am J Physiol* 1999; 276(3 Pt 1): E512-8.
- [45] Haque ME, Leoni L, Zuckerman M, Serai SD, Roman BB. Manganese Enhanced magnetic resonance imaging (MEMRI) of endogenous rodent pancreas activation. 2008; in press.
- [46] Haque ME, Vargas P, Markiewicz E, Dhyani A, Leoni L, La Riviere PJ, *et al.* High resolution and multislice functional MRI of pancreatic β -cell activation. In: *Imaging the Pancreatic β -Cell, 4th Workshop* 2009; 2009; p. 43.
- [47] Antkowiak PF, Tersey SA, Carter JD, Vandsburger MH, Nadler JL, Epstein FH, *et al.* Noninvasive assessment of pancreatic β -cell function *in vivo* with manganese-enhanced magnetic resonance imaging. *Am J Physiol Endocrinol Metab* 2009; 296(3): E573-8.
- [48] Gimi B, Leoni L, Oberholzer J, Braun M, Avila J, Wang Y, *et al.* Functional MR microimaging of pancreatic β -cell activation. *Cell Transplant* 2006; 15(2): 195-203.
- [49] Leoni L, Dhyani A, La Riviere PJ, Roman BB. β -cell subcellular localization of glucose stimulated Mn uptake by X-ray fluorescence: implications for pancreatic MRI. In: *World Molecular Imaging Conference*. Montreal, Canada 2009.
- [50] Brissova M, Powers AC. Revascularization of transplanted islets: can it be improved? *Diabetes* 2008; 57(9): 2269-71.
- [51] Brissova M, Shostak A, Shiota M, Wiebe PO, Poffenberger G, Kantz J, *et al.* Pancreatic islet production of vascular endothelial growth factor--a is essential for islet vascularization, revascularization, and function. *Diabetes* 2006; 55(11): 2974-85.
- [52] Nyman LR, Wells KS, Head WS, McCaughey M, Ford E, Brissova M, *et al.* Real-time, multidimensional *in vivo* imaging used to investigate blood flow in mouse pancreatic islets. *J Clin Invest* 2008; 118(11): 3790-7.
- [53] Morini S, Brown ML, Cicalese L, Elias G, Carotti S, Gaudio E, *et al.* Revascularization and remodelling of pancreatic islets grafted under the kidney capsule. *J Anat* 2007; 210(5): 565-77.
- [54] Medarova Z, Evgenov NV, Dai G, Bonner-Weir S, Moore A. *In vivo* multimodal imaging of transplanted pancreatic islets. *Nat Protoc* 2006; 1(1): 429-35.
- [55] Kriz J, Jirak D, Girman P, Berkova Z, Zacharovova K, Honsova E, *et al.* Magnetic resonance imaging of pancreatic islets in tolerance and rejection. *Transplantation* 2005; 80(11): 1596-603.
- [56] Lu Y, Dang H, Middleton B, Zhang Z, Washburn L, Campbell-Thompson M, *et al.* Bioluminescent monitoring of islet graft survival after transplantation. *Mol Ther* 2004; 9(3): 428-35.
- [57] Medarova Z, Vallabhajosyula P, Tena A, Evgenov N, Pantazopoulos P, Tchivashvili V, *et al.* *In vivo* imaging of autologous islet grafts in the liver and under the kidney capsule in non-human primates. *Transplantation* 2009; 87(11): 1659-66.
- [58] Fowler M, Virostko J, Chen Z, Poffenberger G, Radhika A, Brissova M, *et al.* Assessment of pancreatic islet mass after islet transplantation using *in vivo* bioluminescence imaging. *Transplantation* 2005; 79(7): 768-76.
- [59] Kriz J, Jirak D, White D, Foster P. Magnetic resonance imaging of pancreatic islets transplanted into the right liver lobes of diabetic mice. *Transplant Proc* 2008; 40(2): 444-8.
- [60] Tai JH, Foster P, Rosales A, Feng B, Hasilo C, Martinez V, *et al.* Imaging islets labeled with magnetic nanoparticles at 1.5 Tesla. *Diabetes* 2006; 55(11): 2931-8.
- [61] Denis MC, Mahmood U, Benoist C, Mathis D, Weissleder R. Imaging inflammation of the pancreatic islets in type 1 diabetes. *Proc Natl Acad Sci USA* 2004; 101(34): 12634-9.
- [62] Barnett BP, Arepally A, Karmarkar PV, Qian D, Gilson WD, Walczak P, *et al.* Magnetic resonance-guided, real-time targeted delivery and imaging of magnetocapsules immunoprotecting pancreatic islet cells. *Nat Med* 2007; 13(8): 986-91.
- [63] Beppu H, Maruta K, Kurner T, Kolb H. Diabetogenic action of streptozotocin: essential role of membrane permeability. *Acta Endocrinol (Copenh)* 1987; 114(1): 90-5.
- [64] Kim T, Kim J, Arifin DR, Muja N, Gilad AA, Arepally A, *et al.* Microrfabrication of multifunctional alginate capsule-in-capsules (CICs) for immunoprotected cell transplantation with MR, CT, and US visibility. Abstract Book - *Imaging The Pancreatic β -Cell, 4th Workshop*. Bethesda, MD 2009.
- [65] Jirak D, Kriz J, Strzelecki M, Yang J, Hasilo C, White DJ, *et al.* Monitoring the survival of islet transplants by MRI using a novel technique for their automated detection and quantification. *Magma* 2009; 22(4): 257-65.
- [66] Henquin JC, Cerasi E, Efendic S, Steiner DF, Boitard C. Pancreatic beta-cell mass or beta-cell function? That is the question! *Diabetes Obes Metab* 2008; 10 (Suppl 4): 1-4.
- [67] Lernmark A, Kloppel G, Stenger D, Vathanaprida C, Falt K, Landin-Olsson M, *et al.* Heterogeneity of islet pathology in two infants with recent onset diabetes mellitus. *Virchows Arch* 1995; 425(6): 631-40.
- [68] Moore A, Sun PZ, Cory D, Hogemann D, Weissleder R, Lipes MA. MRI of insulinitis in autoimmune diabetes. *Magn Reson Med* 2002; 47(4): 751-8.
- [69] Billotey C, Asporid C, Beuf O, Piaggio E, Gazeau F, Janier MF, *et al.* T-cell homing to the pancreas in autoimmune mouse models of diabetes: *in vivo* MR imaging. *Radiology* 2005; 236(2): 579-87.
- [70] Medarova Z, Tsai S, Evgenov N, Santamaria P, Moore A. *In vivo* imaging of a diabetogenic CD8+ T cell response during type 1 diabetes progression. *Magn Reson Med* 2008; 59(4): 712-20.
- [71] Henderson JR, Moss MC. A morphometric study of the endocrine and exocrine capillaries of the pancreas. *Q J Exp Physiol* 1985; 70(3): 347-56.
- [72] Bruncardi FC, Stagner J, Bonner-Weir S, Wayland H, Kleinman R, Livingston E, *et al.* Microcirculation of the islets of langerhans. long beach veterans administration regional medical education center symposium. *Diabetes* 1996; 45(4): 385-92.
- [73] Carlsson PO, Flodstrom M, Sandler S. Islet blood flow in multiple low dose streptozotocin-treated wild-type and inducible nitric oxide synthase-deficient mice. *Endocrinology* 2000; 141(8): 2752-7.
- [74] Sandler S, Jansson L, Welsh N. Adaptive response in β -cell function in pancreatic islets isolated from partially pancreatectomized rats. *Mol Cell Endocrinol* 1992; 86(3): 149-56.
- [75] De Paepe ME, Corriveau M, Tannous WN, Seemayer TA, Colle E. Increased vascular permeability in pancreas of diabetic rats: detection with high resolution protein A-gold cytochemistry. *Diabetologia* 1992; 35(12): 1118-24.
- [76] Papaccio G. Early insulinitis and the islet vascular system. *Diabetologia* 1993; 36(7): 682-3.
- [77] Papaccio G. Insulinitis and islet microvasculature in type 1 diabetes. *Histol Histopathol* 1993; 8(4): 751-9.
- [78] Pober JS, Cotran RS. The role of endothelial cells in inflammation. *Transplantation* 1990; 50(4): 537-44.
- [79] Turvey SE, Swart E, Denis MC, Mahmood U, Benoist C, Weissleder R, *et al.* Noninvasive imaging of pancreatic inflammation and its reversal in type 1 diabetes. *J Clin Invest* 2005; 115(9): 2454-61.
- [80] Coenegrachts K, Van Steenberghe W, De Keyzer F, Vanbeckevoort D, Bielen D, Chen F, *et al.* Dynamic contrast-enhanced MRI of the pancreas: initial results in healthy volunteers and patients with chronic pancreatitis. *J Magn Reson Imaging* 2004; 20(6): 990-7.
- [81] Tamada T, Ito K, Sone T, Yamamoto A, Yoshida K, Kakuba K, *et al.* Dynamic contrast-enhanced magnetic resonance imaging of abdominal solid organ and major vessel: comparison of enhancement effect between Gd-EOB-DTPA and Gd-DTPA. *J Magn Reson Imaging* 2009; 29(3): 636-40.
- [82] Haque ME, Xiaobing F, Markiewicz EJ, Leoni L, Roman BB. *In-vivo* manganese enhanced dynamic magnetic resonance imaging (MEDMRI) to evaluate progression of diabetes in rodent pancreas. proceedings of the 17th Annual Meeting of ISMRM. Honolulu, Hawaii, USA 2009.
- [83] Kodama H, Shimojo N, Suzuki KT. Distribution of manganese in rat pancreas and identification of its primary binding protein as pro-carboxypeptidase B. *Biochem J* 1991; 278 (Pt 3): 857-62.

- [84] Dieler AC, Samann PG, Leicht G, Eser D, Kirsch V, Baghai TC, *et al.* Independent component analysis applied to pharmacological magnetic resonance imaging (phMRI): new insights into the functional networks underlying panic attacks as induced by CCK-4. *Curr Pharm Des* 2008; 14(33): 3492-507.
- [85] Escobar J, Pereda J, Arduini A, Sandoval J, Sabater L, Aparisi L, *et al.* Cross-talk between oxidative stress and pro-inflammatory cytokines in acute pancreatitis: a key role for protein phosphatases. *Curr Pharm Des* 2009; 15(26): 3027-42.
- [86] Zhang Y, Ruel M, Beanlands RS, deKemp RA, Suuronen EJ, DaSilva JN. Tracking stem cell therapy in the myocardium: applications of positron emission tomography. *Curr Pharm Des* 2008; 14(36): 3835-53.

Received: December 21, 2009

Accepted: January 18, 2010